THE JOURNAL OF IMMUNOLOGY

This information is current as of June 10, 2013.

CXCL13, CCL21, and CXCL12 Expression in Salivary Glands of Patients with Sjögren's Syndrome and MALT Lymphoma: Association with Reactive and Malignant Areas of Lymphoid Organization

Francesca Barone, Michele Bombardieri, Manuela Maria Rosado, Peter Roger Morgan, Stephen J. Challacombe, Salvatore De Vita, Rita Carsetti, Jo Spencer, Guido Valesini and Costantino Pitzalis

J Immunol 2008; 180:5130-5140; ;
http://www.jimmunol.org/content/180/7/5130

References This article **cites 43 articles**, 19 of which you can access for free at:
http://www.jimmunol.org/content/180/7/5130.full#ref-list-1

Subscriptions Information about subscribing to *The Journal of Immunology* is online at:
http://jimmunol.org/subscriptions

Permissions Submit copyright permission requests at:
http://www.aai.org/ji/copyright.html

Email Alerts Receive free email-alerts when new articles cite this article. Sign up at:
http://jimmunol.org/cgi/alerts/etoc

The Journal of Immunology is published twice each month by
The American Association of Immunologists, Inc.,
9650 Rockville Pike, Bethesda, MD 20814-3994.
Copyright © 2008 by The American Association of Immunologists All rights reserved.
Print ISSN: 0022-1767 Online ISSN: 1550-6606.

Downloaded from http://www.jimmunol.org/ at Univ Studi La Sapienza on June 10, 2013

CXCL13, CCL21, and CXCL12 Expression in Salivary Glands of Patients with Sjögren's Syndrome and MALT Lymphoma: Association with Reactive and Malignant Areas of Lymphoid Organization[1]

Francesca Barone,[2,3]* Michele Bombardieri,[2]*§ Manuela Maria Rosado,[†] Peter Roger Morgan,[¶] Stephen J. Challacombe,[¶] Salvatore De Vita,[‡] Rita Carsetti,[†] Jo Spencer,[‖] Guido Valesini,* and Costantino Pitzalis[4§]

The chemokines (CKs) CXCL13, CCL21, and CXCL12 are known to play differential roles in the organization of the lymphoid tissues and the development of lymphoid malignancies. We investigated the expression of these CKs and their receptors in the salivary glands of Sjogren's syndrome patients with lymphoepithelial lesions (lymphoepithelial sialadenitis or LESA) and in MALT lymphoma to understand their involvement in salivary gland lymphomagenesis. We demonstrate that within salivary glands with LESA and MALT lymphoma the lymphoid CKs CXCL13 and CCL21 are selectively associated with areas of reactive lymphoid proliferation, whereas no significant expression of these molecules was detected in the malignant lymphoid aggregate. Conversely, CXCL12 was observed predominantly in infiltrated ducts and malignant B cells. Accordingly, CXCL13 and CCL21 transcript levels were significantly increased in LESA samples while CXCL12 levels were increased in MALT lymphoma and isolated tumor cells. Low levels of CK receptors were detected on lymphoma-extracted lymphocytes, suggesting down-regulation in the abundance of ligands. Our findings suggest that in salivary gland MALT lymphoma the lymphoid CKs CXCL13 and CCL21 are directly implicated in the organization of ectopic reactive lymphoid tissue, whereas CXCL12 is associated with the infiltrated epithelium and malignant B cell component and is possibly involved in the regulation of malignant B cell survival. ***The Journal of Immunology,*** **2008, 180: 5130–5140.**

The chemokines (CKs)[5] CXCL13, CCL21, and CXCL12 belong to the family of homeostatic CKs, molecules demonstrated to regulate immune and nonimmune cell homing and survival (1–6) as well as the control of lymphoid organogenesis and homeostasis (7). It has been demonstrated that CXCL13 and CCL21 are necessary and sufficient to induce the formation of fully organized lymphoid organs (8–10). Conversely, CXCL12, although involved in lymphoid organ organization and B cell maturation in the bone marrow (11), seems not to be sufficient to induce the formation of mature lymphoid tissue (10).

In chronic inflammatory disorders in humans and mice, the ectopic expression of CXCL13 and CCL21 has been associated with the progressive acquisition of lymphoid features by the inflammatory foci (12). We previously demonstrated that in salivary glands of patients with Sjogren's syndrome (SS), CXCL13 and CCL21 expression is significantly associated with the formation of ectopic lymphoid follicles (13). The functional role of these structures in the selection and expansion of lymphomatous B cell clones in SS has been suggested and these data have been supported by molecular studies showing a clonal relationship between the polyclonal and subsequent monoclonal B cell expansion with progression toward lymphoepithelial lesions (lymphoepithelial sialadenitis or LESA) and lymphoma (14, 15). We recently demonstrated that the presence of these ectopic lymphoid follicles within the salivary glands is significantly associated with expression of the enzyme activation-induced cytidine deaminase (AID) and therefore with the local process of somatic hypermutation and class switch recombination (16). Altogether, these data support the role of ectopic lymphoneogenesis in the development of malignant B cell clones in SS salivary glands, suggesting that lymphoid CKs may also be directly involved in this process.

*Divisione di Reumatologia Dipartimento di Clinica e Terapia Applicata, Università La Sapienza Roma, Rome, Italy; [†]Research Center Ospedale Pediatrico Bambino Gesù, Rome, Italy; [‡]Clinica di Reumatologia, Department of Experimental and Clinical Pathology and Medicine, Università di Udine, Azienda Ospedaliero-Universitaria, Udine, Italy; [§]Centre for Experimental Medicine and Rheumatology, John Vane Science Centre, William Harvey Research Institute, St. Bartholomew's and Royal London School of Medicine, London, United Kingdom; and [¶]Department of Oral Pathology and Oral Medicine at Guy's, St. Thomas and King's College Dental Institute and [‖]Department of Immunobiology, Division of Immunology, Infection and Inflammatory Diseases at Guy's, St. Thomas and King's College School of Medicine, King's College, London, United Kingdom

Received for publication September 6, 2007. Accepted for publication January 27, 2008.

The costs of publication of this article were defrayed in part by the payment of page charges. This article must therefore be hereby marked *advertisement* in accordance with 18 U.S.C. Section 1734 solely to indicate this fact.

[1] This work was supported in part by the educational grants from the Italian Society of Rheumatology and the British Sjögren's syndrome association and from the European Commission Directorate of Research FP-6: Innovative Chemokine-based Therapeutic Strategies for Autoimmunity and Chronic Inflammation. M.B. is recipient of a Clinical Research Fellowship from the Arthritis Research Campaign (grant reference 17132).

[2] F.B. and M.B. contributed equally to this work.

[3] Current address: Department of Immunobiology, Division of Immunology, Infection, and Inflammatory Diseases at Guy's, St. Thomas and King's College, School of Medicine, Guy's Campus, London SE1 9RT, U.K.

[4] Address correspondence and reprint requests to Dr. C. Pitzalis, Centre for Experimental Medicine and Rheumatology, Second Floor, John Vane Science Centre, William Harvey Research Institute, St. Bartholomew's and Royal London School of Medicine, Charterhouse Square, London EC1M 6BQ, U.K. E-mail address: c.pitzalis@qmul.ac.uk

[5] Abbreviations used in this paper: CK, chemokine; AID, activation-induced cytidine deaminase; GC, germinal center; FDC, follicular dendritic cell; HEV, high endothelial venue; LESA, lymphoepithelial sialoadenitis; MALT-L, MALT lymphoma; mSG, minor (labial) salivary gland; MSG, major salivary gland; MZ, marginal zone; PB, peripheral blood; SS, Sjogren's syndrome; PNAd, peripheral node addressin; VFA, volume fraction area; MZ, marginal zone.

Copyright © 2008 by The American Association of Immunologists, Inc. 0022-1767/08/$2.00

Downloaded from http://www.jimmunol.org/ at Univ Studi La Sapienza on June 10, 2013

TABLE I. *Primary and secondary Abs used for immunohistochemistry and FACS analysis*

Clone/Name	Specificity	Host	Source
Primary Abs			
L-26	Human CD20	Mouse	DakoCytomation
A2452	Human CD3	Rabbit	DakoCytomation
1F8	Human CD21	Mouse	DakoCytomation
124	Human bcl-2	Mouse	DakoCytomation
IgD	Human IgD	Rabbit	DakoCytomation
PG-B6p	Human bcl-6	Mouse	DakoCytomation
UCHT1[a]	Human CD3	Mouse	BD Biosciences
HIB19[a]	Human CD19	Mouse	BD Biosciences
ML5[a]	Human CD24	Mouse	BD Biosciences
2A3[a]	Human CD27	Mouse	BD Biosciences
HB7[a]	Human CD38	Mouse	BD Biosciences
L17F12[a]	Human CD5	Mouse	BD Biosciences
HI10a[a]	Human CD10	Mouse	BD Biosciences
UCHL-1[a]	Human CD45RO	Mouse	BD Biosciences
FN50[a]	Human CD69	Mouse	BD Biosciences
1A10	Human CD31	Mouse	Novocastra Laboratories
MECA-79	Human/mouse PNAd	Rat	BD Pharmingen
AF801	Human CXCL13	Goat	R&D Systems
AF366	Human CCL21	Goat	R&D Systems
AF310	Human CXCL12	Mouse	R&D Systems
51505.111	Human CXCR5	Mouse	R&D Systems
12G5	Human CCR7	Mouse	BD Biosciences
3D12	Human CXCR4	Mouse	BD Biosciences
Secondary Abs			
Rabbit anti-rat biotin	Rat Ig	Rabbit[b]	DakoCytomation
Goat anti-mouse biotin	Mouse Ig	Goat[b]	DakoCytomation
Rabbit anti goat biotin	Goat Ig	Rabbit[b]	DakoCytomation

[a] FITC, PE, PE coupled to cyanine dye Cy7TM (PE-Cy7), allophycocyanin, allophycocyanin coupled to cyanine dye Cy7TM (allophycocyanin-Cy7), and cytochrome-labeled Abs were used.
[b] Biotinylated.

Interestingly, a key role for CXCL12 in the migration and survival of Ab-secreting plasma cells (17) and malignant B cells has been recently provided that proposes CXCL12 as being a "molecular bridge" between autoimmunity and lymphoid malignancy development (18).

In this work we characterize CXCL13, CCL21, and CXCL12 expression in LESA and in the reactive and malignant components of MALT lymphomas (MALT-Ls) at both the mRNA and the protein levels. We show that CXCL13 and CCL21 expression selectively associates with the reactive component of the lymphoid proliferation, whereas wide and aberrant CXCL12 expression is present on ductal epithelial cells and in malignant B cells. The differential distribution of these CKs in different functional microenvironments within the tumor suggests that these molecules play very diverse roles in the dynamic development of lymphoma formation in chronic inflammatory conditions. CXCL13 and CCL21 association with the reactive foci supports a direct involvement of these molecules in maintaining the ongoing local Ag-driven polyclonal B cell activation. In contrast, the expression of CXCL12 on the epithelium and in the malignant B cells suggests a role for this CK in the migration, organization, and possibly the survival and maturation of lymphomatous B cells.

Materials and Methods

Patients and samples

SS minor salivary gland (mSG) biopsies from 12 patients (10 females and two males) with a mean age of 57.1 years (range 33–69), a focus score of >1 (19), four SS major salivary gland (MSG) specimens with the diagnosis of LESA (3 female, 1 male, mean age of 52.1 years and a range of 48–56 years), and 20 SS MSGs specimens from patients with non-Hodgkin B cell MALT-L (18 females, 2 males, mean age of 55.4 years and a range of 30–74 years), were obtained from the tissue bank of the Oral Pathology Department at Guy's Hospital (London, U.K.). Patients were diagnosed with SS according to the revised American-European criteria (20). MSG and mSG biopsies were conducted for routine diagnostic purposes following the patient's consent as approved by the Guy's Hospital Research Ethics Committee (LREC 05/Q0702/1). κ- and λ-chain staining and PCR analysis for Ig L chain restriction were performed at the time of the diagnosis.

Immunohystochemistry

Antibodies. A list of primary and secondary Abs is reported in Table I.

Histological characterization of SS minor and MSGs, MALT-L samples, and relationship with CK expression. Immune cell infiltrates, high endothelial venule (HEV) formation, and CK expression in SS minor and MSGs and SS MALT-L samples were characterized by immunohistochemistry staining of sequential sections. After rehydration, formalin-fixed sections underwent Ag retrieval using Target retrieving solution or proteinase K (DakoCytomation). Sections were double stained for CD3/CD20 (T/B cell segregation), CD20/IgD (follicular B cells), and CD21/bcl-2 (follicular dendritic cell (FDC) networks to identify germinal centers (GCs)) using the EnVision Doublestain System (DakoCytomation). For single staining (peripheral node addressin (PNAd), bcl-6, CXCL13, CCL21, and CXCL12) after Ag unmasking and endogenous biotin blocking (avidin-biotin blocking system (DakoCytomation)), sections were rinsed and incubated with appropriate biotinylated secondary Abs and then with streptavidin-biotin complex-alkaline phosphatase (DakoCytomation). Color reaction was developed using Vector Red (Vector Laboratories) and sections were counterstained with hematoxilin. Isotype-matched control Abs were used as a negative control. For mSG foci characterization, the histological score system that we have previously described (13) was applied.

Downloaded from http://www.jimmunol.org/ at Univ Studi La Sapienza on June 10, 2013

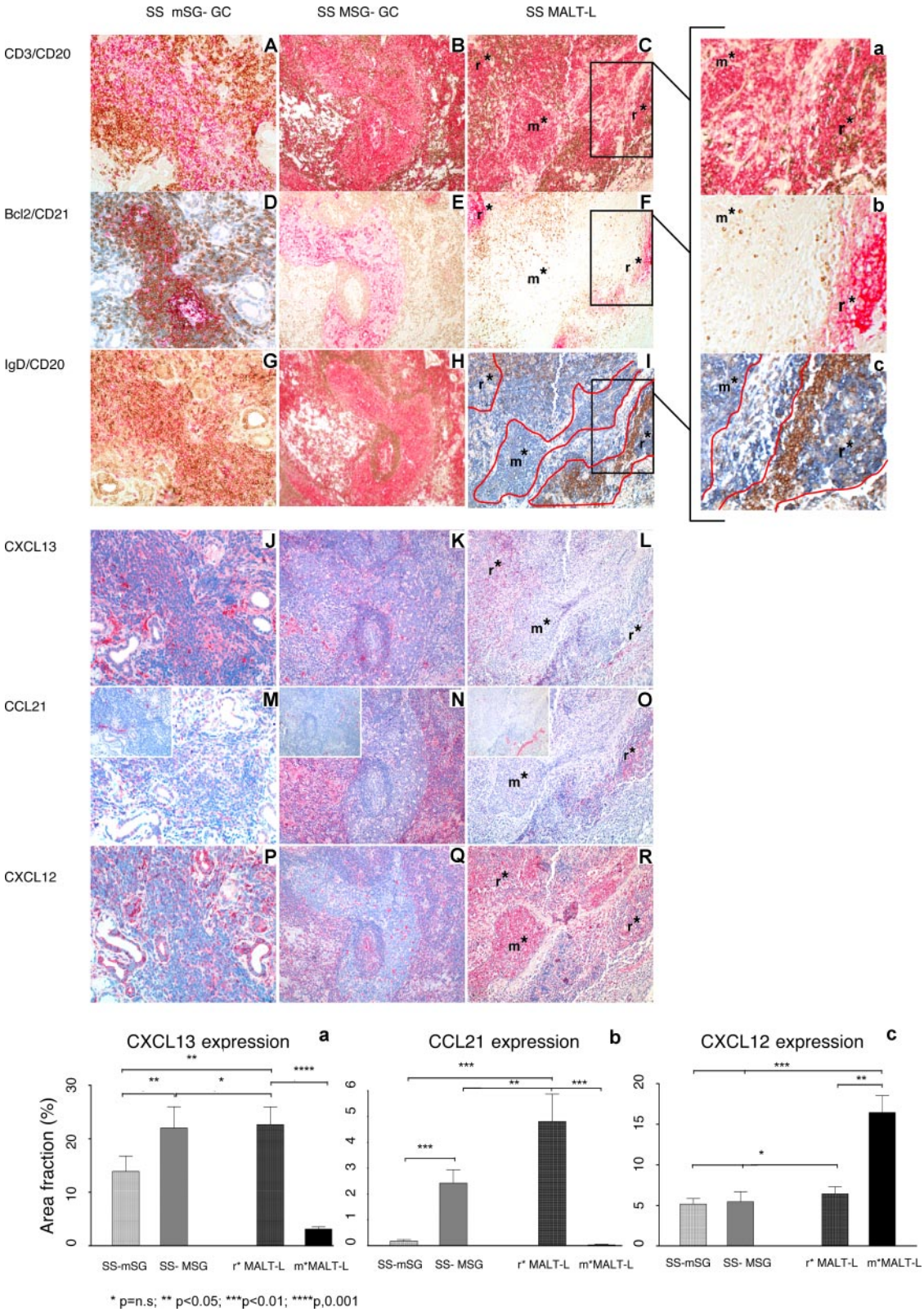

FIGURE 1. Characterization of cellular infiltrate and CK expression in SS mSGs, SS MSGs, and SS MALT-Ls. Photomicrographs of 3-μm-thick sections of human SS mSGs, SS MSGs, and SS MALT-Ls were double stained for CD3 (brown) and CD20 (purple) (*A–C*; to detect B/T cell segregation), bcl-2 (brown) and CD21 (purple) (*D–F*; to detect germinal center and mantle zone), IgD (brown) and CD20 (purple in *G* and *H* and blue in *I*; to detect follicular B cells). Sequential section analysis of ectopic GCs in SS mSG (*left column, A*, *D*, and *G*) and in SS-MSG (*second column from left*, *B*, *E*, and *H*) showing the acquisition of lymphoid features with T/B cell segregation (*A* and *B*), presence of a FDC network within the GC (*D* and *E*), evidence of mantle zone $CD20^+IgD^+$ follicular B cells and $CD20^+IgD^-$ MZ-like B cells (brown and purple, respectively, in *G* and *H*). Sequential section analysis of a SS-MALT-L (*third column, C*, *F*, and *I*) was performed in which is evident the presence of reactive areas (r*) characterized by lymphoid features similar to those described for SS minor and major gland foci (*C*, *F*, and *I* and particularly in *Ca*, *Fb*, and *Ic*) in close association but physically separated from residual ducts infiltrated by monocytoid-like ($IgD^-CD20^+bcl\text{-}2^+$) malignant (m*) B cells (purple in *C* and blue in *I*). FDC networks are detected in close contact with the ducts (purple in *F* and *Fb*), but no IgD^+ follicular B cells (brown)

Downloaded from http://www.jimmunol.org/ at Univ Studi La Sapienza on June 10, 2013

Quantification of CK expression was performed using a computerized image acquisition and analysis system connected to an Olympus BX60 microscope (analySIS; Soft Imaging Systems). Dimensionally calibrated digital images of the stained sections for CXCL13, CXCL12, and CCL21 performed on eight mSGs, four MSGs with LESA, and 12 MALT-Ls were analyzed by thresholding positive staining in detected areas of interest. Digital image analysis estimated the CK volume fraction area (VFA) as the ratio of the CK positive area to total area analyzed. Infiltrated and normal ducts were excluded from the analysis.

Identification of CK producing cells. Double staining for CXCL13, CCL21, CXCL12, CD20, CD3, and CD68 was performed to histologically identify the cell production source of the CKs of interest within SS MSGs by using the Dako EnVision Doublestain system (DakoCytomation) according to the manufacturer' instructions as previously described (13).

Cell isolation, flow cytometry analysis, and cell sorting

Mononuclear cells were isolated from two SS MALT-L parotid glands following enzymatic digestion as previously described (21). Briefly, parotid tissue was minced into fragments in petri dishes containing alkaline medium (RPMI 1640, 5% FCS, 1% L-glutamine, and 1% penicillin/streptomycin; Sigma-Aldrich). Fragments were dissociated into single cells following sequential 30-min incubations in digestion medium (alkaline medium plus 5 mM CaCl2 and 1 mg/ml collagenase H (Sigma-Aldrich)) at 37°C with continuous stirring. After each incubation step the cells were passed through a 70-μm pore size nylon cell strainer (BD Falcon) and resuspended in basic medium containing 2% FCS. Dissociated cells were pooled together and leukocytes were purified by Ficoll-Paque Plus (Amersham Biosciences) gradient and stained for FACS analysis.

Mononuclear cells from peripheral blood, parotid glands, and lymph node were stained with the appropriate combination of fluorescent primary and secondary Abs (Table I) followed by streptavidin-Red 670, streptavidin-allophycocyanin (Caltag Laboratories). Dead cells were excluded from analysis by side/forward scatter gating. All analyses were performed on a FACSCanto flow cytometer (BD Biosciences) interfaced to FACSDiva 4.2.0 software.

Mononuclear cells from peripheral blood (two healthy donors) and two parotid glands were stained for CD3 and CD19 and purified by cell sorting using the FACSVantage SE sorter (BD Biosciences) interfaced to PC FACS Digital Vantage 2.1.2 software. Sorted cells, purity >99%, were resuspended in RNA later (Ambion) and stored at −80°C.

Real time PCR analysis

Total RNA was extracted from parotid glands (two SS MSGs, three SS MALT-Ls one normal parotid gland, two parotid carcinomas, and 1 lymph node) using the Qiagen RNeasy mini kit. First-strand cDNA was synthesized using ThermoScript RT-PCR System (Invitrogen Life Technologies). For quantitative TaqMan real-time evaluation of CXCL13, CCL21, and CXCL12 transcripts, specific primers and probes were used (Table I). The real-time PCR was run using the ABI PRISM 7900HT instrument and relative quantification was measured using the Comparative C_T (Threshold Cycle) Method. The cDNA from a normal human lymph node was used as calibrator.

Statistical analysis

Differences in quantitative variables among multiple groups were analyzed by a Kruskal-Wallis test followed by Dunn's posthoc test to compare the differences between each variable. All statistical analyses were performed using GraphPad Prism version 3.03 for Windows (GraphPad Software). $p < 0.05$ was considered statistically significant.

Results

Histomorphological analysis identifies diverse B cell subpopulations in SS minor and MSGs with malignant features in MALT-Ls.

In SS mSGs the periductal inflammatory foci characterized by a high degree of lymphoid organization (Fig. 1, *A*, *D*, and *G*), previously defined as grade 3 foci (13), were observed in proximity to mostly normal or partially infiltrated ducts (13, 22). In contrast, many SS MSGs with LESA and all SS MALT-L were characterized by a largely subverted glandular structure with acinar and ductal loss and diffuse lymphomonocytoid infiltrate. Within the major glands and lymphomas, two distinct areas of cellular organization with particular histological features were distinguishable: follicular reactive (r*) and malignant (m*) areas (Fig. 1).

Follicular structures were characterized by T/B cell segregation. Histologically detectable GCs were found in 100% of the samples analyzed. These areas in LESAs (Fig. 1, *B*, *E*, and *H*) and MALT-Ls (Fig. 1, boxed areas containing r* in *C*, *F*, and *I* and shown at a higher magnification in *Ca*, *Fb*, and *Ic*) were identified as the reactive areas of the lymphoid infiltration. These structures were mainly inhabited by follicular $CD20^+IgD^+bcl\text{-}2^+$ B cells (Fig. 1*H* and r* in *I* and I*c*) resembling the organization of SS reactive foci (13). Physically separated from these areas, a second diverse B cell population ($CD20^+IgD^-bcl\text{-}2^+$) was detected. This population formed the main component of the lymphomatous samples (Fig. 1, m* in *C*, *F*, and *I* and at a higher magnification in *Ca*, *Fb*, and *Ic*). In MALT-L this population was characterized by peculiar histological features (pale nuclei, evident nucleoli, and frequent mitotic figures) and was organized in dense sheets of monocytoid-like B cells, subverting the glandular structure and disaggregating the ducts (Fig. 1, m* in *C* and *I* and in *Ca* and *Ic*). On the base of the morphological features and surface Ags this population was histologically identified as the MALT-L malignant or m* component.

CXCL13 preferentially associates with the reactive lymphoid infiltration within LESA and SS MALT-L MSGs

As previously demonstrated (13), within SS minor glands CXCL13 expression is strongly associated with the degree of lymphoid organization of the foci (Fig. 1*J*).

Similarly, a high density of $CXCL13^+$ cells was detected in 100% of the SS MSGs and the SS MALT-Ls analyzed in strict association with $CD20^+IgD^+$ and $CD21^+$ FDC-rich areas (Fig. 1*K*) in the reactive areas (Fig. 1*L*, r*). In contrast, little CXCL13 expression was detected within the malignant areas and ducts infiltrated by $CD20^+IgD^-$ marginal zone (MZ)-like B cells (Fig. 1*L*, m*).

Such differential expression of CXCL13 within each sample was quantified by using image analysis as described in *Materials and Methods*. A significant increase in CXCL13 VFA was observed in both SS MSGs and SS MALT-L reactive areas in comparison with SS mSG follicular areas as seen by the percentages of VFA (mean ± SEM): 22 ± 3.9 vs 13.9 ± 2.9 ($p < 0.05$) and 22.6 ±

appear to populate the malignant area (*I* and *Ic*). CXCL13 (purple in *J*, *K*, and *L*) localizes in the B cell-rich area of the SS-mSG and SS-MSG foci (purple in *J* and *K*) as well as the MALT reactive area (r* in *L*). Diffuse CXCL13 staining can be detected in FDC-rich areas within GC, whereas intense $CXCL13^+$ cells populate the $CD20^+IgD^+$ follicular B cell-rich mantle zone in SS-MSGs and MALT reactive areas (*K* and r* in *L*). Virtually no $CXCL13^+$ cells are detected in the $CD20^+IgD^-$ malignant B cell-infiltrated duct (m* in *L*). Little CCL21 (purple in *M*, *N*, *O*) is present in the T cell-rich area in SS mSGs in exclusive association with PNAd expression on HEVs (*M*, with $PNAd^+$ vessel in the *inset*). Abundant CCL21 expression is in the wide SS MSGs follicles and in the MALT-L T cell-rich area not restricted to $PNAd^+$ vessels (*N* and *inset* and r* in *O*). No evident CCL21 expression is detected within the malignant B cell infiltrated duct (m* in *O*). Intense CXCL12 expression (purple in *P*, *Q*, and *R*) in ducts and is within infiltrating cells in a representative SS mSGs focus (*P*). Intense $CXCL12^+$ cells within a FDC^+ GC in SS-MSGs (*Q*) and extremely intense CXCL12 staining within the reactive and malignant areas in MALT-Ls (r* and m* in *R*) are shown. Original magnification (*A*–*R*) was ×100. In the graphs, quantitative evaluations of CXCL13 (*a*), CCL21 (*b*), and CXCL12 (*c*) staining in eight SS mSGs, four SS-MSGs, and 12 MALT-L reactive (r*) and malignant (m*) areas are shown in the graphs. See *Results* for detailed results and statistical analysis. Bars represent the mean ± SEM.

Downloaded from http://www.jimmunol.org/ at Univ Studi La Sapienza on June 10, 2013

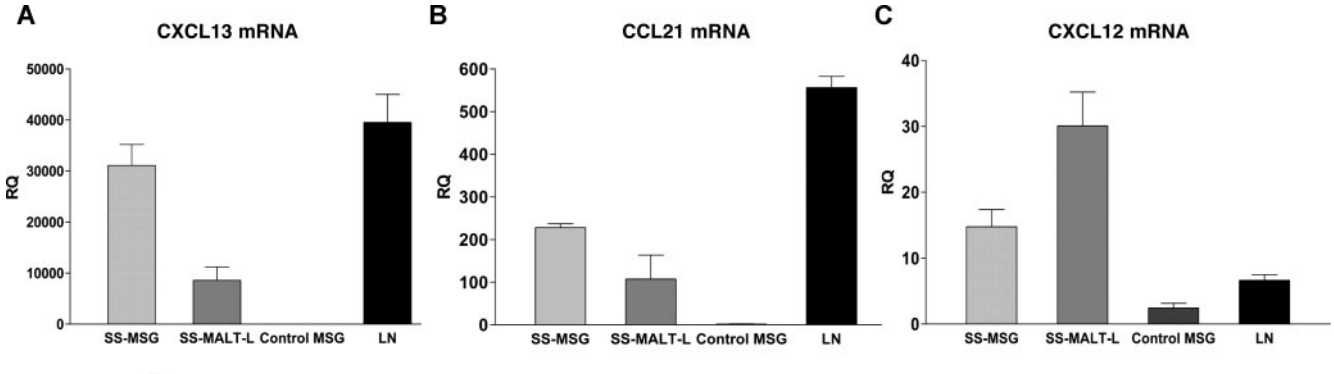

D

Patient	CXCL13 mRNA	CCL21 mRNA	CXCL12 mRNA
SS-MSG 1	35,179	245	18.1
SS-MSG 2	27,000	209	11.8
SS-MALT 1	9,821	131	37.7
SS-MALT 2	7,496	104	32.3
SS-MALT 3	8,421	78.4	20.3
Control MSG 1	6.8	2.1	3.4
Control MSG 2	3.1	1.6	2.8
Control MSG 3	1.0	1.0	1.0
Lymph node (LN)	39,500	556	6.8

Data are expressed as relative quantification (RQ) using one of the control (MSG 3) as calibrator (=1)

FIGURE 2. CK transcript analysis in SS MSGs with LESA and MALT-Ls. Quantitative TaqMan real-time PCR evaluation of CXCL13 (*A*), CCL21 (*B*), and CXCL12 (*C*) transcript levels in whole nonlymphomatous major (parotid glands) salivary glands of two patients with SS (SS-MSGs), three with SS-MALT-Ls, and three control parotid glands with a human lymph node (LN) shown for comparison. *A* and *B*, Transcript levels of CXCL13 and CCL21 were strongly increased in reactive SS-MSGs in comparison with controls (~30,000- and ~400-fold, respectively, for CXCL13 and CCL21) and with MALT-L (30- and 2-fold increases in the reactive samples). *C*, Conversely, CXCL12 transcript analysis demonstrated a higher level of CXCL12 mRNA in SS-MALT-L samples as compared with controls (~30-fold increase) and to reactive SS-MSGs (~2-fold increase). The low expression of CCL21 mRNA (*B*) and the strong expression of CXCL12 mRNA (*C*), but not CXCL13 mRNA (*A*), in control parotid glands relate to the constitutive expression of CCL21 and CXCL12 by salivary gland lymphatic vessels and ducts, respectively. Data are expressed as relative quantification (RQ) with bars representing the mean and SEM of each group. *D*, Table illustrating the mean of the mRNA (RQ) levels calculated for each sample analyzed.

3.3 vs 13.9 ± 2.9 ($p < 0.05$), respectively (Fig. 1*a*). Importantly, a strong difference was detected in CXCL13 expression within MALT reactive areas as compared with malignant areas (22.6 ± 3.3 vs 3.1 ± 0.4 ($p < 0.001$), Fig. 1*a*) providing quantitative confirmatory data of CXCL13 preferential distribution.

CCL21 is overexpressed in SS MSGs and MALT-L and is associated with the reactive T cell areas

Within the T cell area of SS mSG grade 3 foci, CCL21 was poorly expressed and only in association with $PNAd^+$ HEVs (Fig. 1*M* and *inset*). On the contrary, within the major glands and in MALT-L samples CCL21 was abundantly expressed in all of the samples analyzed and selectively confined to the enlarged T cell compartment of the reactive areas (Fig. 1, *B* and *N* and r* in *C* and in *O* with *inset*). No CCL21 expression was observed within the infiltrated ducts and in MALT-L malignant areas where the B cells were predominant (Fig. 1, m* in *C* and *O* with *inset*).

In line with this observation, quantitative image analysis showed a progressive increase in the CCL21 VFA in SS major glands and SS-MALT-L reactive areas as compared with SS mSG foci (2.4 ± 0.5 vs 0.2 ± 0.05 ($p < 0.01$) and 4.2 ± 1.1 vs 0.2 ± 0.05 ($p < 0.01$), respectively; Fig. 1*b*). Also, a significant increase in CCL21 expression was detected in reactive SS-MALT-L vs SS major gland reactive areas ($p < 0.05$). In addition, image analysis data confirmed the virtual absence of CCL21 expression (0.03 ± 0.02; Fig. 1*b*) within the malignant areas of SS MALT-L.

Increase in CXCL12 expression is associated with the inflammatory reactive infiltrate but also with malignant cells in MALT-Ls

Within SS mSG foci we detected a discrete CXCL12 expression on ductal epithelial cells and vessels and within the FDC-rich areas (Fig. 1*P*). A similar pattern was also observed within reactive and lymphomatous major glands where diffuse and intense CXCL12

Downloaded from http://www.jimmunol.org/ at Univ Studi La Sapienza on June 10, 2013

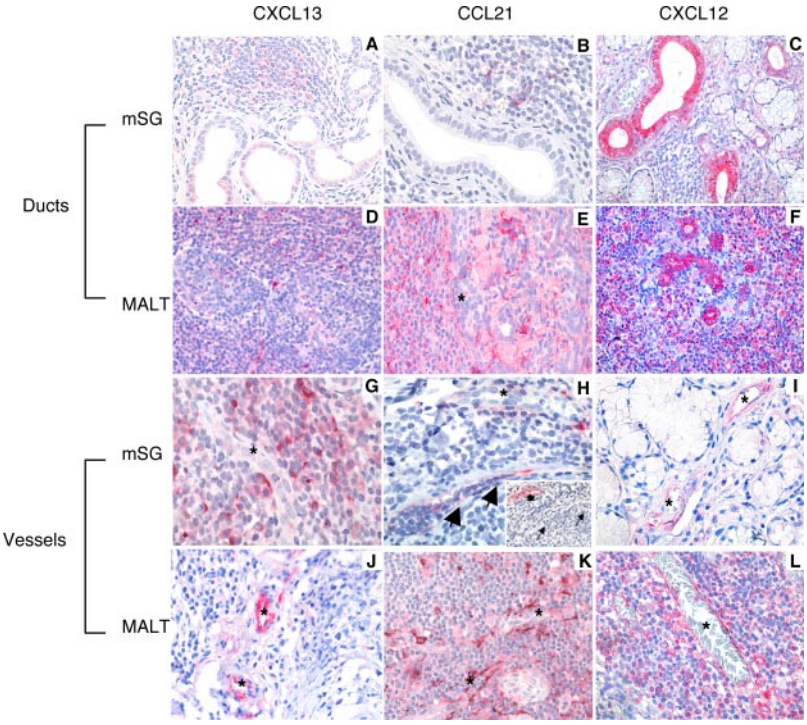

FIGURE 3. Differential epithelial and vascular patterns of CXCL13, CCL21, and CXCL12 expression in SS mSGs and SS MALT-Ls. Photomicrographs of 3-μm-thick sections immunohistochemical staining of CXCL13 (purple in *A*, *D*, *G*, and *J*), CCL21 (purple in *B*, *E*, *H*, and *K*), and CXCL12 (purple in *C*, *F*, *I*, and *L*) in SS-mSGs and SS-MALT-Ls. Weakly positive CXCL13 staining was observed in ductal structures in both SS-mSGs and SS-MALT-Ls (*A* and *D*). No CCL21 expression was observed in SS-mSG ducts (*B*) or in a residual duct in SS-MALT-L (*E*, asterisk). Intense CXCL12 staining on ductal epithelial cells is observed both in SS-mSGs (*C*) and SS-MALT-L (*F*). Vascular analysis shows no endothelial CXCL13 expression in SS-mSGs (*G*, asterisk), whereas strong CXCL13 expression is detected within vessels in SS-MALT-L (*J*, *asterisks*). CCL21 expression in the T cell area of SS-mSGs (*H*) is exclusively associated with PNAd$^+$ HEVs (purple; *inset*, asterisk, and arrows), and in MALT lymphoma (*K*, asterisk) CXCL12 vascular expression is detectable in both SS-mSG and SS-MALT-L (*I* and *L*, asterisks). Original magnification was $\times$10 in *A*, *C*, *D*, *E*, *F*, *J*, and *L*, $\times$20 in *B*, *K*, and *I*, and $\times$40 in *G*, *H*, and *L*.

expression was detected within the GCs (Fig. 1, *Q* and *R*). Interestingly, and in contrast with CXCL13 and CCL21, CXCL12 expression was strongly detected in MALT-Ls also within the infiltrated ducts and in areas of malignant (CD20$^+$IgD$^-$ B cell proliferation (Fig. 1, m* in *R*). Image analysis confirmed these observations, showing a significant difference in CXCL12 expression within SS MALT-L malignant areas as compared with MALT reactive areas, SS mSGs, and SS MSGs (16.5 $\pm$ 2.1 for SS-MALT malignant vs 5.2 $\pm$ 0.6 for reactive and 5.5 $\pm$ 1.2 for SS mSGs ($p < 0.01$ in both cases) and 6.4 $\pm$ 0.8 for SS MSGs ($p < 0.05$); Fig. 1*c*).

Differential CXCL13, CCL21, and CXCL12 transcript levels in SS MSG and SS MALT-Ls confirm the preferential expression observed by immunohistology

RT-PCR analysis performed on mRNA extracted from total parotid glands confirmed a higher level of CXCL13 production within SS MSGs as compared with SS MALT-L, although a significant increase compared with controls was still detected (Fig. 2*A*). Similarly, we showed higher level of CCL21 mRNA production in SS MSGs with LESA as compared with SS MALT-L and controls, where a modest constitutive expression of the molecule was detectable as shown previously (23) (Fig. 2*B*). These results correlate with the histological observation that CXCL13 and CCL21 are predominantly expressed in the reactive infiltrate in SS MSGs with LESA as compared with MALT-L, where the malignant infiltration was characterized by the virtual absence of the two CKs.

Conversely and again in keeping with the histological observations, CXCL12 mRNA production was more prominent in SS MALT-L as compared with reactive SS MSGs, confirming abundant CXCL12 expression in areas of malignant B cell infiltration. CXCL12 transcript levels in SS MALT- lymphoma were increased ~30-fold as compared with controls where strong expression of CXCL12 mRNA was detected, reflecting constitutive CXCL12 production by ductal epithelial cells (24) (Fig. 2*C*).

Differential CXCL13, CCL21, and CXCL12 expression in epithelial and vascular structures in SS minor and MSGs and MALT-L

Epithelial expression of CXCL13 and CCL21 was negligible on the ductal structures identified in minor and major MALT-L glands (Fig. 3, *A* and *D* and *B* and *E*). On the contrary, strong CXCL12 expression was detected on the ductal epithelium (Fig. 3, *C* and *F*). In SS mSGs (Fig. 3*G*) we could not detect any CXCL13 vascular expression. Interestingly, however, CXCL13$^+$ vessels were easily identifiable in MSGs and MALT-L (Fig. 3*J*).

With regard to CCL21 expression, it was consistently detected in all SS tissues (minor and MSGs and in MALT-L) in association with PNAd$^+$ HEVs (Fig. 3, *B*, *E*, *H*, and *K*) although, as already discussed, within the major glands a widely diffuse CCL21 expression was observed in the enlarged T cell area (Fig. 3, *H* and *K*). Strong CCL21 expression was observed on lymphatic vessels (Fig. 3*H*) as we previously published (13).

Strong expression of CXCL12 was also consistently observed on the vascular and lymphatic endothelium of both SS mSGs (Fig. 3*I*) and SS MSGs and in SS MALT-L (Fig. 3*L*).

Monocyte-derived cells produce lymphoid CKs in reactive areas of SS-MALT-L: autocrine and paracrine production of CXCL12 by ducts and malignant B cells

The majority of CXCL13- and (to a lesser extent) CCL21-producing cells are characterized by an abundant, elongated cytoplasm and pale large nuclei, morphologically resembling monocytes/macrophages (Fig. 4, *A* and *C*). A minority of the CXCL13$^+$ cells also display a lymphocytic morphology. Within the GCs, diffuse CXCL13 expression appears to colocalize with the presence of CD21$^+$ FDC cells (Fig. 1, *E* and *K*). Double staining with CD68/CXCL13 and CD68/CCL21 also demonstrated that a high number of CXCL13 and, to a lesser extent, CCL21$^+$ cells belong to the monocytic/macrophage lineage (CD68$^+$) (Fig. 4, *B* and *D*). In addition, in MALT-L a large proportion of CCL21$^+$ cells was

Downloaded from http://www.jimmunol.org/ at Univ Studi La Sapienza on June 10, 2013

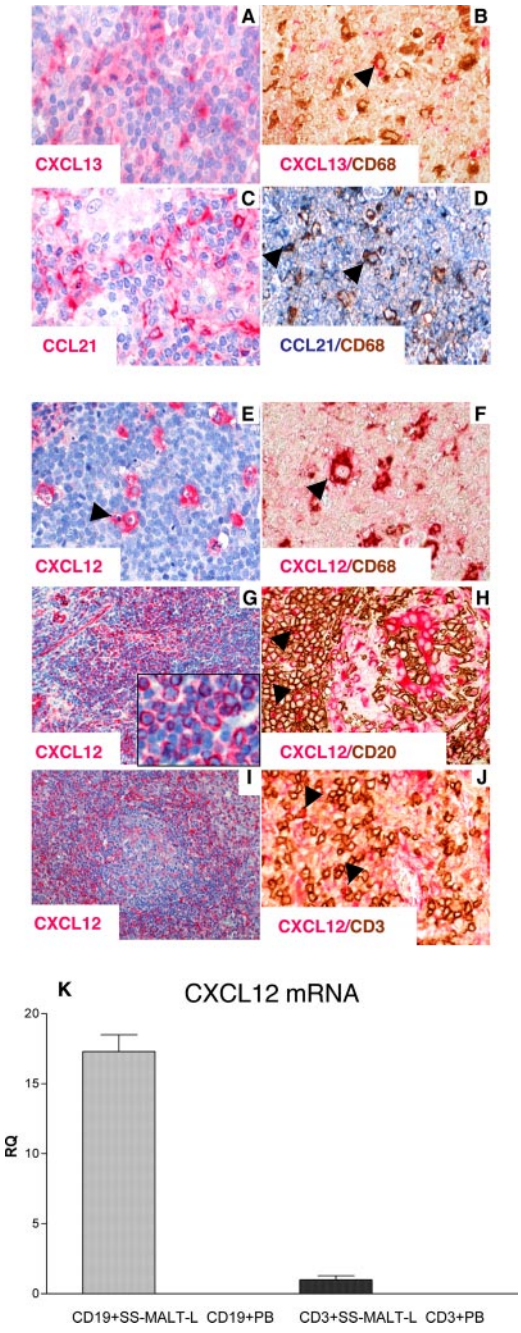

FIGURE 4. Monocyte-derived cells express CXCL13, CCL21, and CXCL12 in the reactive areas of SS-MALT-L samples. CXCL12 production by ductal epithelial cells and lymphomatous B cells in SS-MALT-Ls is shown. Representative immunohistochemistry for CXCL13 (purple in *A* and *B*), CCL21 (purple in *C* and blue in *D*), and CXCL12 (purple in *E–J*) in single (*A*, *C*, *E*, *G*, and *I*) and double staining with CD68 (brown in *B*, *D*, and *F*), CD20 (brown in *H*), and CD3 (brown in *J*) was performed on 3-μm-thick sections of a MALT-L sample. *A–G*, Within the reactive areas most CXCL13$^+$ cells showed a large cytoplasm (*A*) and were double stained for CD68 (*B*, arrow), confirming the monocyte-derived origin of these cells. CCL21$^+$ cells showed a dendritic cell-like morphology (*C*) and partial overlap with CD68 in the T cell area (*D*, arrows). Within the reactive GC of MALT-L, CXCL12 was detected in large cells with dense chromatin aggregates (*E* arrow) that were demonstrated to be CD68$^+$ tingible body macrophages (*F*, arrow). Diverse CXCL12$^+$ populations in the malignant area colocalize with ductal epithelial cells, vessels, and malignant B cells as shown by morphological appearance (*G*; in single staining and at higher magnification in the *inset*). *H*, Representative CXCL12/CD20 double staining in a malignant area of SS-MALT-L demonstrates physical contact between malignant B cells infiltrating the ducts (brown) and the epithelial cells positive for CXCL12 (purple). Of note, some of the B cells are positive for the CK (arrows). *I*, CXCL12 in a reactive GCs showing intense CXCL12 staining in the FDC rich areas and the mantle zone but also in the T cell area. *J*, CXCL12/CD3 double staining demonstrates CXCL12 expression also by infiltrating CD3$^+$ T cells (arrows). Original magnification was $\times$10 for *G* and *I*, $\times$20 for *A–D*, *H*, and *J*, and $\times$40 for *E* and *F*. *K*, Diagram showing quantitative TaqMan real-time PCR evaluation of CXL12 transcript levels in CD19- and CD3-sorted cells from a parotid gland sample SS-MALT-L and from PB of two normal donors. Strong CXCL12 mRNA expression was detected on CD19$^+$ B lymphocytes isolated from SS-MALT-L but not from the PB of normal controls, where CXCL12 was undetectable, supporting the histological evidence of CXCL12 expression by malignant B cells within SS-MALT-L. Lower but still detectable CXCL12 mRNA expression was also observed in CD3$^+$ T lymphocytes from SS-MALT-L parotid gland but not from normal PB. Data are expressed as relative quantification (RQ) using the expression of CXCL12 mRNA in the T cell population as calibrator (=1), with bars representing the mean and SEM of the triplicates for each sample. See *Results* for detailed results.

identified by morphology and distribution as resident stromal cells (Fig. 4*C*). CXCL13 and CCL21 double staining with CD20 or CD3 failed to clarify whether lymphocytes represent a source of the two CKs in MALT-Ls because intimate physical contact between CD20$^+$IgD$^+$ and CXCL13$^+$ cells and CD3$^+$ and CCL21$^+$ cells was consistently detected, making the histological analysis difficult to interpret (data not shown). Nonetheless, RT-PCR analysis performed on isolated T and B lymphocytes showed a negligible production of CXCL13 from infiltrating T and B cells (although upregulated compared with normal PBMCs; data not shown) that was inadequate to explain the high transcript levels of the molecule detected in the total MALT-Ls (Fig. 2*A*). No expression of CCL21 on sorted MALT-L and peripheral blood (PB) CD3$^+$ and CD19$^+$ cells was detected.

Within the GCs of SS MALT-L and SS MSGs, CXCL12$^+$ cells were characterized by dense dark aggregates of chromatin and large cytoplasms; these cells express CD68 and were identified as tingible body macrophages (Fig. 4, *E* and *F*). Conversely, within the malignant infiltrate high levels of CXCL12 were expressed by a large number of small monocytoid-like cells positive for CD20, identified as the malignant component of the B infiltration (Fig. 4, *G* and *H*). Accordingly, high levels of CXCL12 mRNA were detected in CD19$^+$ lymphocytes isolated from SS MALT-L but not in PB CD19$^+$ sorted cells (Fig. 4*K*). Low levels of CXCL12 at both the protein (Fig. 4, *I* and *J*) and mRNA levels (Fig. 4*K*) were detected in MALT-L isolated T cells.

Characterization of B and T cell subsets and CXCR5, CCR7, and CXCR4 expression on isolated SS MALT-L cells

To identify the expression of CK receptors in the diverse lymphoid populations infiltrating MALT-L, we analyzed mononuclear cells isolated from the parotid glands and one regional lymph node of two patients undergoing radical surgery as well as normal PBMCs used as controls. Isolated B cells from the two samples of SS-MALT-L showed diverse stages of B cell maturation (transitional, mature, and memory B cells) with clear different proportions in SS-MALT-Ls as compared with cells from a regional lymph node (not shown) and normal PBMCs (Fig. 5*A*). In addition, within the MALT-Ls, but not in the controls, we could detect a MZ-like B cell population (CD19$^+$CD24$^-$CD27^{low}; Fig. 5*A*) and CD5$^-$CD10$^-$ (data not shown) consistent with the dominant B cell malignant population within the lymphomas. The FACS profile for one of the two patients is illustrated in Fig. 5. CXCR5 analysis on B cells

Downloaded from http://www.jimmunol.org/ at Univ Studi La Sapienza on June 10, 2013

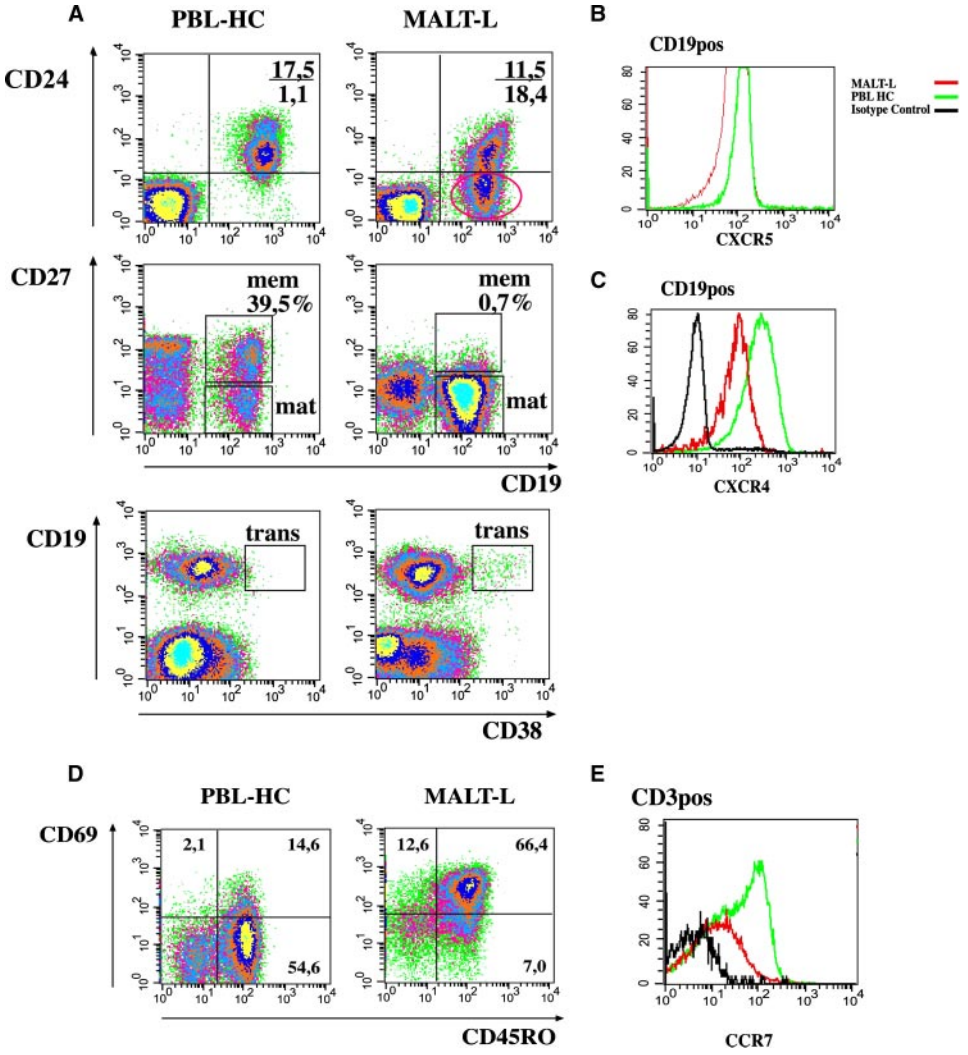

FIGURE 5. Characterization of MALT-L-extracted lymphocytes and CK-R expression on MALT lymphoma (MALT-L)-extracted B and T lymphocytes. Peripheral blood lymphocytes from healthy control (PBL-HC) and lymphocytes extracted from one major salivary gland from a patient with MALT lymphoma (MALT-L) were stained with Abs to CD24, CD27, CD19, CD38, CD3, CD69, and CD45RO to identify B cell subpopulations and to characterize the T cells infiltrating the glands (*A* and *D*). Staining for CXCR5, CXCR4, and CCR7 was performed on isolated B (CXCR5 and CXCR4 in *B* and *C*) and T cells (CCR7 on T cells *E*), respectively. *A*, Values indicate the frequency of $CD19^+CD24^+$ cells (*upper right*) and $CD19^+CD24^-$ cells (*lower right*) in the lymphocyte gate. Note that $CD19^+CD24^-$ (circled in red) are rare or absent in healthy donors; thus, this population in this MALT-L patient may represent tumor cells. (*A*, middle row) Plots representing the frequency of mature (mat) and memory (mem) B cells, showing enrichment in mature B cells in the MALT-L compared with the controls. Of note, a low number of infiltrating $CD27^+$ memory B cells and a low number of transitional (trans) B cells were detected in the tumor-extracted lymphocytes. *B*, Histogram represents CXCR5 expression on gated $CD19^+$ (CD19pos) cells from PBL-HC and one MALT-L. Note the tendency of the MALT-L-extracted lymphocytes in down-modulating cell surface expression of CXCR5 (red line). *C*, Plots representing the expression of CXCR4 and CD19 in the lymphocyte gate, showing CXCR4 down-regulation on MALT-extracted $CD19^+$ cells. *D*, Gated CD3 cells; values indicate the frequency of naive activated ($CD69^+CD45RO^-$), memory-activated ($CD45RO^+CD69^+$), and memory ($CD45RO^+CD69^-$) $CD3^+$ cells. Note the higher percentage of activated and mature T cells in MALT-Ls. *E*, Histogram represents the CCR7 down-regulation in $CD3^+$ (CD3+) T cells, the salivary gland profile from one MALT-L patient in red, and peripheral blood lymphocytes from healthy controls in green.

demonstrated that, although most parotid gland-extracted lymphocytes express CXCR5, a fraction of these cells down-modulate the receptor (Fig. 5*B*, red line). Similarly, significant CXCR4 down-modulation in MALT-L-extracted lymphocytes was detected (Fig. 5*C*, red line), likely reflecting receptor down-regulation upon in vivo CXCL12 ligation.

Naive T cells were detected within the extracted population, although the majority of the infiltrating T cells in both samples display a memory phenotype ($CD45RO^+$). Moreover the majority of T cells showed a pronounced activated phenotype as documented by the strong up-regulation of CD69 compared with controls (Fig. 5*D*). As expected and in keeping with the above phenotype, CCR7 expression was clearly reduced (Fig. 5*E*, red line).

Discussion

In this study we demonstrated for the first time that the ectopic expression of CXCL13, CCL21, and CXCL12 in MSGs of SS patients with LESA and MALT-L identifies diverse microenvironments of immune cell aggregation within the glands. We showed selective expression of CXCL13 and CCL21 in association with areas of reactive lymphoid proliferation inhabited by $CD20^+IgD^+$ follicular B cells organized in GCs with $CD21^+$ FDC networks and the formation of $PNAd^+$ HEVs. Conversely, strong expression

Downloaded from http://www.jimmunol.org/ at Univ Studi La Sapienza on June 10, 2013

of CXCL12 was demonstrated in MALT-L (and to lesser extent in LESA MZ-B cells) in areas characterized by the presence of wide malignant areas of $CD20^+IgD^-$ MZ-like B cells organized in sheets of monocytoid-like cells with nuclear atypias and frequent mitotic figures infiltrating the parenchyma, often colonizing the follicles (25) and subverting the glandular structure. We demonstrated that within the reactive areas $CD68^+$ cells expressed the three CKs; however, ductal epithelial cells and malignant cells were solely responsible for CXCL12 expression in the malignant areas. We finally provided evidence that CXCL13, CCL21, and CXCL12 receptors are expressed on MALT-L-isolated B and T lymphocytes, although at low levels as compared with normal B and T lymphocytes, suggesting that the ligand/receptor axis of these CKs is functionally involved in the SS lymphomagenesis.

In recent years a large number of studies have shown that B cell lymphoma development, unique among neoplasms, is more dependent on the functional interaction of the neoplastic cells with the ongoing immune response in local microenvironments rather than by the intrinsic proliferative properties of the malignant B cells (26). This is particularly evident in MALT lymphomas arising in areas of chronic inflammation (i.e., within the stomach during *Helicobacter pylori*-induced gastritis), where Ag-driven lymphoid proliferation precedes the development of MALT-L and lymphoma remission follows Ag eradication (27). In SS, there are data suggesting that an Ag-driven immune response takes place in association with ectopic GCs (28). Moreover, convincing evidence on the presence of a clonal relationship between Ag-driven polyclonal lymphoid reaction and monoclonal proliferation leading to the malignant expansion has been recently provided (14, 29). On this basis, SS MALT-Ls are believed by some authorities to be MZ-B cell lymphomas that display hypermutated Ig genes compatible with a post-GC derivation (30). In this context we demonstrated selective AID expression in association with GC-like structure (and presence of a CD21 long isoform) in SS and in MALT-L but not in areas infiltrated by malignant B cells (16). Altogether, these data suggest that malignant B cell clones, having undergone somatic hypermutation and class switch recombination, escape from the same ectopic GCs responsible for the reactive local Ag-driven immune response and migrate in the epithelium where they give rise to the characteristic lymphoepithelial lesions.

In this context, we provided evidence of the pivotal role of CXCL13 and CCL21 in the organization and maintenance of ectopic tertiary lymphoid structures under chronic inflammatory conditions (31) and in particular in SS (13). Accordingly, within LESA and SS MALT lymphoma samples we invariably identified highly organized ectopic GCs associated with strong expression of CXCL13 and CCL21 within compartmentalized B and T cell areas. These aberrant lymphoid structures, similar to the inflammatory foci in SS, were consistently detected in association with infiltrated ducts and that believed to represent a continuous and excessive source of auto-Ags for the GC reaction. Within these areas, both in LESA and MALT-L, CXCL13-abundant expression displays a similar distribution to that observed in SS mSGs (13), being diffusely expressed in colocalization with $CD21^+$ FDCs and by $CD68^+$ cells in association with $CD20^+IgD^+$ follicular B cells.

Surprisingly, within the wide malignant areas of SS MALT-L mainly populated by $CD20^+IgD^-bcl\text{-}2^+$ MZ-like B cells, a negligible amount of CXCL13 was detected by immunohistochemistry. A similar distribution of CXCL13 in association with $CD20^+IgD^+$ follicular B cells rather than MZ B cells has been described in the spleen (32), where other molecules are known to chemoattract MZ B cells (33). Our RT-PCR analysis results support these data, showing increased CXCL13 transcripts in SS MSGs where the reactive follicular B cell component was more represented as compared with MALT-Ls. These data are in contrast to a previous study on *H. pylori*-induced gastric MALT-L that reported CXCL13 expression on malignant B cells identified by morphological appearance (34). However, our histological observations are supported by RT-PCR analysis of MALT-L-isolated B lymphocytes that showed only a negligible amount of CXCL13 in MALT lymphoma-extracted $CD19^+$ cells. In addition to the obvious possible technical explanations (different histological methodology) for this discrepancy, it is possible to hypothesize that functional differences in gastric and salivary gland MALT-L malignant B cells may be involved in determining a differential expression of CXCL13. In this regard it is known that lymphoid CK expression is regulated by the NF-κB system (7) and that several translocations (such as t (11;18)(q21;q21) and t (14;18)(q32;q21)) involving NF-κB genes have been described in MALT-Ls arisen in various tissues (26). At present, there is no consistent evidence of common translocations in gastric, ocular, and parotid lymphomas, thus raising the possibility that diverse alterations in the NF-κB pathway may results in differential CXCL13 transcription in malignant B cells from MALT-Ls from diverse sites.

Another important aspect that has emerged is that gastric MALT lymphoma B cell proliferation is critically dependent on the presence of tumor-extracted, activated Ag-specific T cells (35). In this context, new evidence on the functional role of CCL21 in enhancing Ag-specific cell proliferation and CD69 up-regulation in T lymphocytes has recently been provided (36), together with the demonstration of CD69 involvement in the arrest of activated lymphocytes in secondary lymphoid organs (37). In this study we demonstrated that in SS MSGs and MALT-Ls a strong up-regulation of CCL21 takes place in correlation with the presence of a high number of $CD69^+$ activated T cells infiltrating the glands. These data suggest a prominent role for CCL21 in salivary gland lymphomagenesis in the recruitment and chronic activation of $CD62L^+CCR7^+$ naive and/or central memory T cells that, once stimulated, provide within the reactive areas the stimuli for the expansion and survival of Ag-specific B cells.

Thus, coordinated CXCL13 and CCL21 actions in the reactive areas of the major glands appear to reproduce the amplificatory loop already described at sites of physiological lymphoid neogenesis, where lymphoid CKs chemoattract lymphotoxin-$\alpha\beta$-producing cells that, in turn, induce CK production (7).

We have previously demonstrated AID expression in association with the GCs of MALT-Ls but not in areas infiltrated by malignant B cells (16). This finding suggests a functional link between the ectopic lymphoid structures where the B cells clones are educated toward the locally displayed Ag and the malignant clones infiltrating the epithelium. It has been recently reported that AID expression is associated with aberrant somatic hypermutation leading to the activation of protooncogenes in large B cell lymphomas and MALT-Ls (38). In this article we suggest that CXCL13 and CCL21 expression, within the same reactive area positive for AID, regulates within the glands the formation and maintenance of the lymphoid structures functional for the generation of autoreactive B cells clones implicated in MALT lymphomagenesis.

The most interesting result in this work is related to the expression of CXCL12. This CK is known to exert a wide range of angiogenetic, homeostatic, chemoattractant, immunoregulatory, and inflammatory effects. In this article we have demonstrated intense CXCL12 expression in SS samples with LESA and MALT-L. CXCL12 was expressed in the reactive area where we demonstrated that $CD68^+$ tingible body macrophages, scavengers of apoptotic centrocytes, represent the major source of CXCL12 in ectopic CGs, implying a possible aberrant involvement of CXCL12 in the regulation of the life/death balance in ectopic GCs.

Downloaded from http://www.jimmunol.org/ at Univ Studi La Sapienza on June 10, 2013

However, the more intense CXCL12 was detected in the malignant areas. In the lymphoepithelial lesion in MALT-L and LESA samples we showed a physical contact between CXCL12-producing ductal epithelial cells and infiltrating MZ-like B cells. The functional role of CXCL12 in the migration, survival, and metastatic spread of epithelial and hematopoietic malignancies has been extensively described (39). In these cases, the principal source of CXCL12 was identified in the mesenchymal and bone marrow-derived cells within the tumors (40), suggesting that the aberrant reproduction of a nurse cell microenvironment contributes to the development and persistence of these malignancies (41). Moreover, the role of CXCL12 in the migration and survival of Ab-secreting plasma cells has been long known (17). In the present study we suggest that the ductal epithelial cells provide a similar microenvironment for mature Ag-experienced MZ-like B cells in the salivary glands, supporting the migration, survival, and in few cases the possible maturation toward the plasma cell fate of this population.

In addition to the strong ductal expression of CXCL12 we demonstrated, at both the mRNA and protein levels, that SS-MALT-L-isolated B cells produce abundant CXCL12. In agreement with this increased CXCL12 expression, we demonstrated a significant down-regulation of CXCR4 on MALT-L isolated B lymphocytes that is likely to be the result of CXCR4 internalization upon CXCL12 ligation (42). Although no CXCL12 expression has been detected on normal B cells, CXCL12 expression on CNS lymphomatous cells has been recently reported (43) and, more recently, CXCL12 has been demonstrated to be capable of sustaining hematopoietic malignant B cell survival (18).

In this article we demonstrated that the CXCL12/CXCR4 axis is likely to be functional in MALT-L malignant cells and that the epithelial structures and the same malignant B cells can produce this CK. Altogether these findings suggest that, after undergoing Ag selection and clonal expansion in the lymphoid structures organized by CXCL13 and CCL21, lymphomatous B cells clones are provided with signals of survival and proliferation by the same ductal epithelial cells that provide them with the antigenic stimulation. In this scenario, the evidence that the same malignant B cells can produce CXCL12 might reflect a further step in lymphomagenesis where the malignant clones acquire an additional degree of independence from the microenvironment, providing themselves with survival signals.

These data are in line with the hypothesis that MALT clones maturate their affinity in the GC and undergo expansion outside of these structures (16). Additional experiments aimed at clarifying the functional role of CXCL12 in the survival and spreading of the lymphomatous B cells are currently being performed in our laboratory.

In conclusion, in this study we demonstrated that the differential expressions of CXCL13, CCL21, and CXCL12 within SS salivary glands with LESA and MALT-L regulate diverse functional microenvironments of lymphoid organization, respectively orchestrating the reactive lymphoid areas that favor the perpetuation of the immune response and the malignant areas where expansion and proliferation of the B cell clones take place.

Acknowledgments

We gratefully thank Prof. Peter G. Isaacson, Department of Pathology, Royal Free and University College Medical School, London, U.K. for revision of the SS-MALT-L samples and for help in the characterization of malignant marginal zone B cells within MALT-L.

Disclosures

The authors have no financial conflict of interest.

References

1. D'Apuzzo, M., A. Rolink, M. Loetscher, J. A. Hoxie, I. Clark-Lewis, F. Melchers, M. Baggiolini, and B. Moser. 1997. The chemokine SDF-1, stromal cell-derived factor 1, attracts early stage B cell precursors via the chemokine receptor CXCR4. *Eur. J. Immunol.* 27: 1788–1793.
2. Aiuti, A., I. J. Webb, C. Bleul, T. Springer, and J. C. Gutierrez-Ramos. 1997. The chemokine SDF-1 is a chemoattractant for human $CD34^+$ hematopoietic progenitor cells and provides a new mechanism to explain the mobilization of $CD34^+$ progenitors to peripheral blood. *J. Exp. Med.* 185: 111–120.
3. Ansel, K. M., V. N. Ngo, P. L. Hyman, S. A. Luther, R. Forster, J. D. Sedgwick, J. L. Browning, M. Lipp, and J. G. Cyster. 2000. A chemokine-driven positive feedback loop organizes lymphoid follicles. *Nature* 406: 309–314.
4. Luther, S. A., H. L. Tang, P. L. Hyman, A. G. Farr, and J. G. Cyster. 2000. Coexpression of the chemokines ELC and SLC by T zone stromal cells and deletion of the ELC gene in the plt/plt mouse. *Proc. Natl. Acad. Sci. USA* 97: 12694–12699.
5. Salvucci, O., L. Yao, S. Villalba, A. Sajewicz, S. Pittaluga, and G. Tosato. 2002. Regulation of endothelial cell branching morphogenesis by endogenous chemokine stromal-derived factor-1. *Blood* 99: 2703–2711.
6. Broxmeyer, H. E., L. Kohli, C. H. Kim, Y. Lee, C. Mantel, S. Cooper, G. Hangoc, M. Shaheen, X. Li, and D. W. Clapp. 2003. Stromal cell-derived factor-1/CXCL12 directly enhances survival/antiapoptosis of myeloid progenitor cells through CXCR4 and Gαi proteins and enhances engraftment of competitive, repopulating stem cells. *J. Leukocyte Biol.* 73: 630–638.
7. Mebius, R. E. 2003. Organogenesis of lymphoid tissues. *Nat. Rev. Immunol.* 3: 292–303.
8. Luther, S. A., T. Lopez, W. Bai, D. Hanahan, and J. G. Cyster. 2000. BLC expression in pancreatic islets causes B cell recruitment and lymphotoxin-dependent lymphoid neogenesis. *Immunity* 12: 471–481.
9. Chen, S. C., G. Vassileva, D. Kinsley, S. Holzmann, D. Manfra, M. T. Wiekowski, N. Romani, and S. A. Lira. 2002. Ectopic expression of the murine chemokines CCL21a and CCL21b induces the formation of lymph node-like structures in pancreas, but not skin, of transgenic mice. *J. Immunol.* 168: 1001–1008.
10. Luther, S. A., A. Bidgol, D. C. Hargreaves, A. Schmidt, Y. Xu, J. Paniyadi, M. Matloubian, and J. G. Cyster. 2002. Differing activities of homeostatic chemokines CCL19, CCL21, and CXCL12 in lymphocyte and dendritic cell recruitment and lymphoid neogenesis. *J. Immunol.* 169: 424–433.
11. Allen, C. D., K. M. Ansel, C. Low, R. Lesley, H. Tamamura, N. Fujii, and J. G. Cyster. 2004. Germinal center dark and light zone organization is mediated by CXCR4 and CXCR5. *Nat. Immunol.* 5: 943–952.
12. Aloisi, F., and R. Pujol-Borrell. 2006. Lymphoid neogenesis in chronic inflammatory diseases. *Nat. Rev. Immunol.* 6: 205–217.
13. Barone, F., M. Bombardieri, A. Manzo, M. C. Blades, P. R. Morgan, S. J. Challacombe, G. Valesini, and C. Pitzalis. 2005. Association of CXCL13 and CCL21 expression with the progressive organization of lymphoid-like structures in Sjogren's syndrome. *Arthritis Rheum.* 52: 1773–1784.
14. Gasparotto, D., S. De Vita, R. De, V. A. Marzotto, G. De Marchi, C. A. Scott, A. Gloghini, G. Ferraccioli, and M. Boiocchi. 2003. Extrasalivary lymphoma development in Sjogren's syndrome: clonal evolution from parotid gland lymphoproliferation and role of local triggering. *Arthritis Rheum.* 48: 3181–3186.
15. Martin, T., J. C. Weber, H. Levallois, N. Labouret, A. Soley, S. Koenig, A. S. Korganow, and J. L. Pasquali. 2000. Salivary gland lymphomas in patients with Sjogren's syndrome may frequently develop from rheumatoid factor B cells. *Arthritis Rheum.* 43: 908–916.
16. Bombardieri, M., F. Barone, F. Humby, S. Kelly, M. McGurk, P. Morgan, S. Challacombe, V. S. De, G. Valesini, J. Spencer, and C. Pitzalis. 2007. Activation-induced cytidine deaminase expression in follicular dendritic cell networks and interfollicular large B cells supports functionality of ectopic lymphoid neogenesis in autoimmune sialoadenitis and MALT lymphoma in Sjogren's syndrome. *J. Immunol.* 179: 4929–4938.
17. Hargreaves, D. C., P. L. Hyman, T. T. Lu, V. N. Ngo, A. Bidgol, G. Suzuki, Y. R. Zou, D. R. Littman, and J. G. Cyster. 2001. A coordinated change in chemokine responsiveness guides plasma cell movements. *J. Exp. Med.* 194: 45–56.
18. Burger, M., T. Hartmann, M. Krome, J. Rawluk, H. Tamamura, N. Fujii, T. J. Kipps, and J. A. Burger. 2005. Small peptide inhibitors of the CXCR4 chemokine receptor (CD184) antagonize the activation, migration, and antiapoptotic responses of CXCL12 in chronic lymphocytic leukemia B cells. *Blood* 106: 1824–1830.
19. Chisholm, D. M., and D. K. Mason. 1968. Labial salivary gland biopsy in Sjogren's disease. *J. Clin. Pathol.* 21: 656–660.
20. Vitali, C., S. Bombardieri, R. Jonsson, H. M. Moutsopoulos, E. L. Alexander, S. E. Carsons, T. E. Daniels, P. C. Fox, R. I. Fox, S. S. Kassan, et al. 2002. Classification criteria for Sjogren's syndrome: a revised version of the European criteria proposed by the American-European Consensus Group. *Ann. Rheum. Dis.* 61: 554–558.
21. Mega, J., J. R. McGhee, and H. Kiyono. 1992. Cytokine- and Ig-producing T cells in mucosal effector tissues: analysis of IL-5- and IFN-γ-producing T cells, T cell receptor expression, and IgA plasma cells from mouse salivary gland-associated tissues. *J. Immunol.* 148: 2030–2039.
22. Bombardieri, M., F. Barone, V. Pittoni, C. Alessandri, P. Conigliaro, M. Blades, R. Priori, I. McInnes, G. Valesini, and C. Pitzalis. 2004. Increased circulating levels and salivary gland expression of interleukin-18 in patients with Sjogren's syndrome: relationship with autoantibody production and lymphoid organization of the periductal inflammatory infiltrate. *Arthritis Res. Ther.* 6: R447–R456.

Downloaded from http://www.jimmunol.org/ at Univ Studi La Sapienza on June 10, 2013

23. Willimann, K., D. F. Legler, M. Loetscher, R. S. Roos, M. B. Delgado, I. Clark-Lewis, M. Baggiolini, and B. Moser. 1998. The chemokine SLC is expressed in T cell areas of lymph nodes and mucosal lymphoid tissues and attracts activated T cells via CCR7. *Eur. J. Immunol.* 28: 2025–2034.
24. Amft, N., S. J. Curnow, D. Scheel-Toellner, A. Devadas, J. Oates, J. Crocker, J. Hamburger, J. Ainsworth, J. Mathews, M. Salmon, et al. 2001. Ectopic expression of the B cell-attracting chemokine BCA-1 (CXCL13) on endothelial cells and within lymphoid follicles contributes to the establishment of germinal center-like structures in Sjogren's syndrome (see comments). *Arthritis Rheum.* 44: 2633–2641.
25. Isaacson, P. G., A. C. Wotherspoon, T. Diss, and L. X. Pan. 1991. Follicular colonization in B-cell lymphoma of mucosa-associated lymphoid tissue. *Am. J. Surg. Pathol.* 15: 819–828.
26. Isaacson, P. G., and M. Q. Du. 2004. MALT lymphoma: from morphology to molecules. *Nat. Rev. Cancer* 4: 644–653.
27. Wotherspoon A. C., C. Dogliosi, T. C. Diss, L. Pan, A. Meschini, and M. De Boni. 1993. Regression of primary low grade B cell gastric lymphoma of mucosa associated lymphoid tissue type after eradication of *Helicobacter pylori*. *Lancet* 342: 575–577.
28. Stott, D. I., F. Hiepe, M. Hummel, G. Steinhauser, and C. Berek. 1998. Antigen-driven clonal proliferation of B cells within the target tissue of an autoimmune disease: the salivary glands of patients with Sjogren's syndrome. *J. Clin. Invest.* 102: 938–946.
29. Bahler D. W., and S. H. Swerdlow. 1998. Clonal salivary gland infiltrates associated with myoepithelial sialadenitis (Sjogren's syndrome) begin as nonmalignant antigen-selected expansions. *Blood* 91: 1864–1872.
30. Bahler D. W., J. A. Miklos, and S. H. Swerdlow. 1997. Ongoing Ig gene hypermutation in salivary gland mucosa-associated lymphoid tissue-type lymphomas. *Blood* 89: 3335–3344.
31. Manzo, A., S. Paoletti, M. Carulli, M. C. Blades, F. Barone, G. Yanni, O. Fitzgerald, B. Bresnihan, R. Caporali, C. Montecucco, et al. 2005. Systematic microanatomical analysis of CXCL13 and CCL21 in situ production and progressive lymphoid organization in rheumatoid synovitis. *Eur. J. Immunol.* 35: 1347–1359.
32. Cyster, J. G., K. M. Ansel, K. Reif, E. H. Ekland, P. L. Hyman, H. L. Tang, S. A. Luther, and V. N. Ngo. 2000. Follicular stromal cells and lymphocyte homing to follicles. *Immunol. Rev.* 176: 181–193.
33. Cinamon, G., M. Matloubian, M. J. Lesneski, Y. Xu, C. Low, T. Lu, R. L. Proia, and J. G. Cyster. 2004. Sphingosine 1-phosphate receptor 1 promotes B cell localization in the splenic marginal zone. *Nat. Immunol.* 5: 713–720.
34. Mazzucchelli, L., A. Blaser, A. Kappeler, P. Scharli, J. A. Laissue, M. Baggiolini, and M. Uguccioni. 1999. BCA-1 is highly expressed in *Helicobacter pylori*-induced mucosa-associated lymphoid tissue and gastric lymphoma. *J. Clin. Invest.* 104: R49–R54.
35. Hussell, T., P. G. Isaacson, J. E. Crabtree, and J. Spencer. 1996. *Helicobacter pylori*-specific tumour-infiltrating T cells provide contact dependent help for the growth of malignant B cells in low-grade gastric lymphoma of mucosa-associated lymphoid tissue. *J. Pathol.* 178: 122–127.
36. Stachowiak, A. N., Y. Wang, Y. C. Huang, and D. J. Irvine. 2006. Homeostatic lymphoid chemokines synergize with adhesion ligands to trigger T and B lymphocyte chemokinesis. *J. Immunol.* 177: 2340–2348.
37. Shiow, L. R., D. B. Rosen, N. Brdickova, Y. Xu, J. An, L. L. Lanier, J. G. Cyster, and M. Matloubian. 2006. CD69 acts downstream of interferon-$\alpha\beta$ to inhibit S1P1 and lymphocyte egress from lymphoid organs. *Nature* 440: 540–544.
38. Deutsch, A. J., A. Aigelsreiter, P. B. Staber, A. Beham, W. Linkesch, C. Guelly, R. I. Brezinschek, M. Fruhwirth, W. Emberger, M. Buettner, et al. 2007. MALT lymphoma and extranodal diffuse large B-cell lymphoma are targeted by aberrant somatic hypermutation. *Blood* 109: 3500–3504.
39. Zlotnik, A. 2004. Chemokines in neoplastic progression. *Semin. Cancer Biol.* 14: 181–185.
40. Burger, J. A., and T. J. Kipps. 2006. CXCR4: a key receptor in the crosstalk between tumor cells and their microenvironment. *Blood* 107: 1761–1767.
41. Kryczek, I., S. Wei, E. Keller, R. Liu, and W. Zou. 2007. Stromal derived factor (SDF-1/CXCL12) and human tumor pathogenesis. *Am. J. Physiol.* 292: C987–C95.
42. Shen, H., T. Cheng, I. Olszak, E. Garcia-Zepeda, Z. Lu, S. Herrmann, R. Fallon, A. D. Luster, and D. T. Scadden. 2001. CXCR-4 desensitization is associated with tissue localization of hemopoietic progenitor cells. *J. Immunol.* 166: 5027–5033.
43. Smith, J. R., K. M. Falkenhagen, S. E. Coupland, T. J. Chipps, J. T. Rosenbaum, and R. M. Braziel. 2007. Malignant B cells from patients with primary central nervous system lymphoma express stromal cell-derived factor-1. *Am. J. Clin. Pathol.* 127: 633–641.

Downloaded from http://www.jimmunol.org/ at Univ Studi La Sapienza on June 10, 2013